Photochemistry and Photobiology, 2017, 93: 642–655

Invited Review

Phytochromes from *Agrobacterium fabrum*†

Tilman Lamparter*[1], Norbert Krauß*[1] and Patrick Scheerer*[2]

[1]Karlsruhe Institute of Technology (KIT), Botanical Institute, Karlsruhe, Germany
[2]Charité – Universitätsmedizin Berlin, Institute of Medical Physics and Biophysics (CC2), Group Protein X-ray Crystallography and Signal Transduction, Berlin, Germany

Received 22 November 2016, accepted 22 February 2017, DOI: 10.1111/php.12761

ABSTRACT

***Agrobacterium fabrum* is a widely used model bacterium for gene transfer from pro- to eukaryote, for genetics and metabolism. The phytochrome system of *Agrobacterium*, encompassing the two phytochromes Agp1 and Agp2, has provided deep insight into phytochrome action in a bacterial organism. This review summarizes recent results on phytochrome evolution, phytochrome regulation of conjugation and plant infection and biochemical studies including the crystal structure of Agp1-PCM, the photosensory core module of Agp1.**

INTRODUCTION

This review about *Agrobacterium* phytochromes is dedicated to Wolfgang Gärtner on the occasion of his 65th birthday. Wolfgang worked in different fields of photobiology. He studied rhodopsins (1), phytochromes (2) and LOV domain proteins (3), among other research fields. After his move from Freiburg to the Max Planck Institute in Mülheim in 1991, where he joined the group of Silvia Braslavsky, the red light photoreceptor phytochrome became his major research topic—after he had been focusing on rhodopsin and bacteriorhodopsin the years before. His research on blue light photoreceptors started later. Initially, Wolfgang's focus was on plant phytochromes. Detailed protocols for large-scale purification of oat phytochrome from the natural source and time-resolved spectroscopy were already established by Silvia Braslavsky (4), and the respective phytochrome samples were used for biophysical studies, for example, by several fast spectroscopy techniques (5–9). The cyanobacterial phytochromes became the second "Standbein" of Wolfgang's phytochrome research (10–15). As a chemist, Wolfgang contributed by synthesis of artificial chromophores for the sake of labeling wherever it was necessary (16,17). Another major contribution was the establishment of recombinant expression of proteins (17). From a current perspective, these are standard techniques in photoreceptor research and there is no more group left which uses purified phytochromes from natural sources. The establishment of recombinant expression, the studies on the photocycle and the use of synthetic chromophores must be regarded as important pioneering work in the field of photoreceptor biochemistry.

Compared to the middle 1990s, our knowledge about phytochrome has now drastically broadened. We know that plant phytochromes enter the nucleus upon photoconversion (18,19). We know a lot more about the roles of plant and fungal phytochromes in signal transduction (20,21). We know that phytochromes exist in algal species which were not commonly known (22,23). We know in which phylogenetic groups phytochromes exist (24) and where they do not exist, for example, in red algae and animals. And we know about photoreceptors with phytochrome-like properties like a special group of chromoproteins in cyanobacteria, called cyanobacteriochromes (25–28). The characteristic feature that led to the discovery of plant phytochromes (29), photoreversibility (see Figs. 1 and 2), holds also for fungal (30), bacterial (31,32), prasinophyte (22), or heterokont (33) phytochromes. The cyanobacteriochromes have copied from canonical phytochromes the principle of a photoreversible switch between two spectrally distinct forms but have modified their spectral features (28,34). However, despite the evolutionary flexibility of the cyanobacteriochromes, in terms of the diversity of spectral features and domain arrangements that can be found within this group of photoreceptors, phytochromes were more successful in eukaryote evolution.

This review is focused on phytochromes Agp1 and Agp2 from *Agrobacterium fabrum* (former: *Agrobacterium tumefaciens*) (32,35). We discuss our work in the context of phytochrome studies on bacterial, cyanobacterial, plant and fungal phytochromes. *Agrobacterium fabrum* is an important model organism for gene transfer from bacterium to plant (36) and many other issues; both its phytochromes can be expressed in recombinant systems in high amounts; these phytochromes are representatives of two major subgroups of phytochromes; and biophysical analyses have provided good insight into their molecular functions. We start off with a discussion on the evolution of phytochromes, which is still an open issue in phytochrome research.

EVOLUTION OF PHYTOCHROMES

Domain arrangements in bacterial, plant and fungal phytochromes are comparable insofar, as the three N-terminal domains are always PAS, GAF and PHY domains. The

*Corresponding authors' emails: tilman.lamparter@kit.edu (Tilman Lamparter), norbert.krauss@kit.edu (Norbert Krauß), and patrick.scheerer@charite.de (Patrick Scheerer)

†This article is a part of the Special Issue dedicated to Dr. Wolfgang Gärtner on the occasion of his 65th birthday.

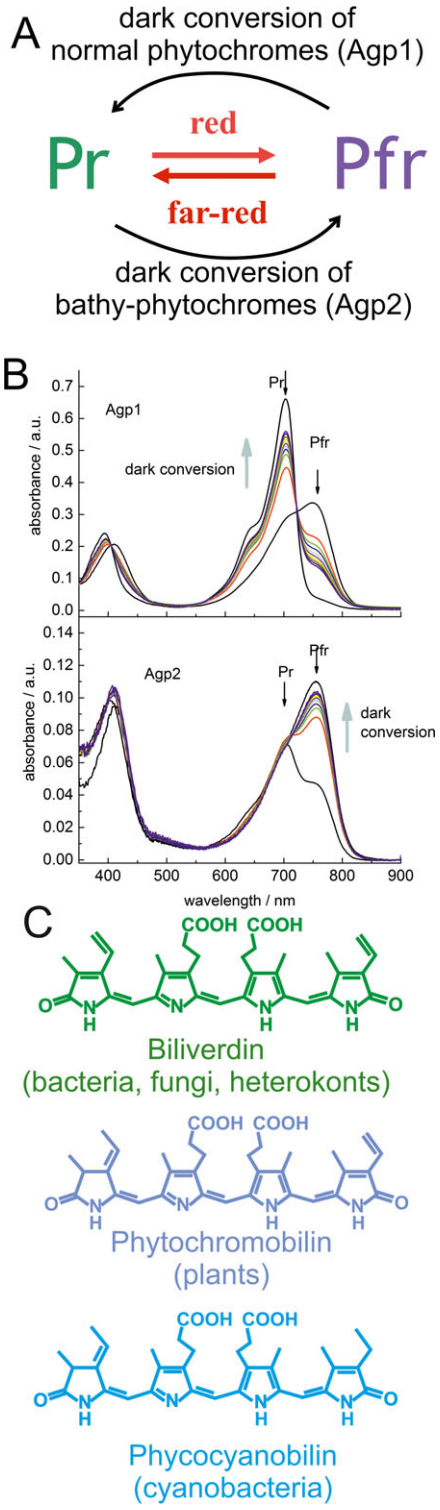

Figure 1. (A) Cartoon describing phytochrome photoreversibility and dark conversion. Bathy phytochromes such as Agp2 undergo dark conversion from Pr to Pfr, typical phytochromes such as Agp1 convert from Pfr to Pr in darkness. Red and far-red light induce Pr-Pfr or Pfr-Pr photoconversion, respectively. (B) Spectra of *Agrobacterium fabrum* Agp1 (above) and Agp2 (below) in the dark adapted forms (Pr and Pfr, respectively), after irradiation (Pfr and Pr dominate, respectively) and during dark incubation. The directions of spectral changes are indicated by arrows. (C) Structures of the bilin chromophores biliverdin, phytochromobilin and phycocyanobilin found in phytochromes. The types of the respective organisms are named in parentheses.

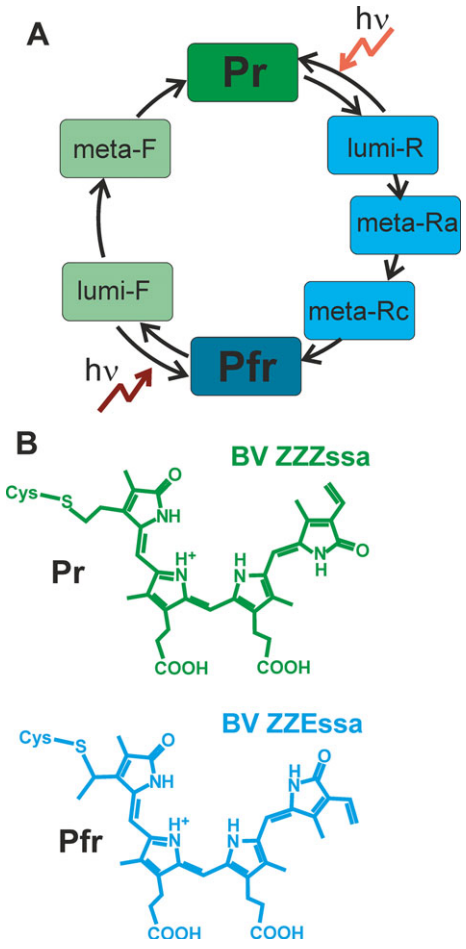

Figure 2. (A) Photocycle intermediates. The first steps of Pr-Pfr and Pfr-Pr photoconversion are light triggered isomerizations. The color code stands for the ZZZ (green) or ZZE (blue) configuration of the chromophore. The intermediate forms are unstable and convert into the subsequent form in light or in darkness. Intermediates have been detected by cryo-trapping or flash photolysis. (B) *ZZZssa* and *ZZEssa* stereochemistry of the biliverdin (BV) chromophore in the Pr and Pfr forms. Cys stands for the covalent chromophore-binding site of the protein. The chromophore is protonated in the Pr and Pfr forms, but transient deprotonation occurs during photoconversion. The two spectrally different forms Pr and Pfr are interconverted by red or far-red light. The fraction of each form is determined by wavelength, intensity and duration of irradiation. Depending on the type of phytochrome, there can be Pfr to Pr or Pr to Pfr dark conversion (in bathy phytochromes).

C-terminal domains are more divergent, and some phytochromes have pronounced N-terminal extensions (see Fig. 3 for domain arrangements of some phytochromes and related proteins). The PAS-GAF-PHY tridomain or photosensory core module (PCM) incorporates the chromophore, undergoes light-induced photoreversible absorbance changes and controls the state of the rest of the protein. The PCM is also the fraction of the entire protein of which several X-ray structures could be obtained. Phylogenetic studies on the overall evolution of phytochromes are most often based on PCM sequences.

Although such studies provide many clear results, they also leave several open issues, such as the evolutionary origin of eukaryotic phytochromes. The amino acid sequences of bacterial phytochromes are very diverse; the most distantly related sequences have amino acid identities of 15%. This broad diversity is combined with diverse domain arrangements. The major

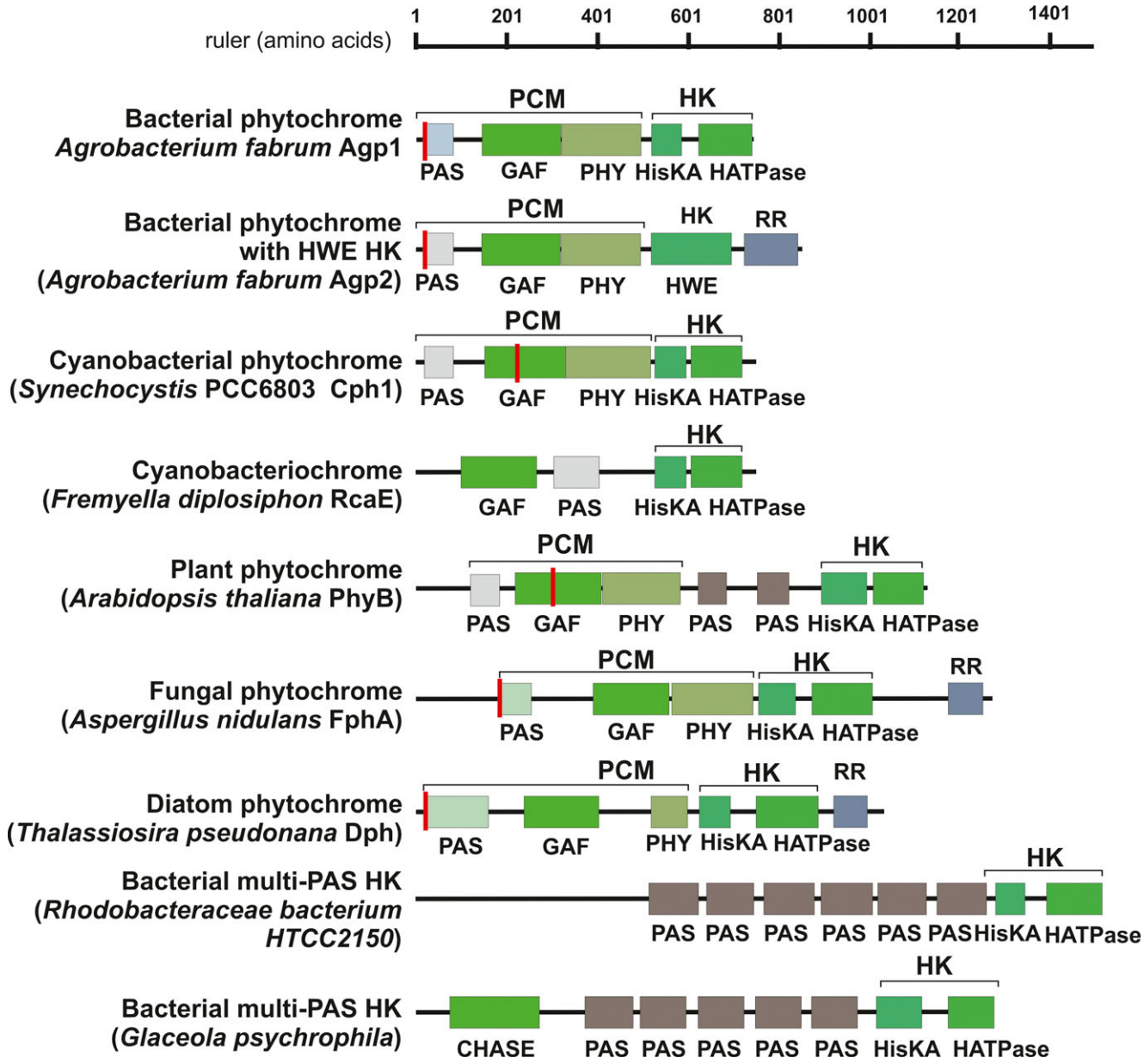

Figure 3. Domain arrangements of phytochromes and related proteins. The PCM of phytochromes (indicated above each chart) consists of GAF, PAS and PHY domains. Most often the C-terminal region is a histidine kinase (HK, indicated above the chart). Histidine kinases usually have two domains, one substrate and dimerization domain (HisKA) and one ATPase region (HATPase). In plant phytochromes, the histidine kinase is dysfunctional. Two PAS domains separate the histidine kinase from the PCM in plant phytochromes. A response regulator (RR, indicated above each chart) is part of the polypeptide in some bacterial phytochromes with HWE histidine kinases, such as Agp2, in fungal and in diatom phytochromes. The domain arrangement of a cyanobacteriochrome, RcaE, is shown for comparison. The two proteins shown on the bottom are examples for multiple PAS domains combined with histidine kinases. The positions of the chromophore-binding Cys residues are indicated by vertical red lines.

domain pattern of bacterial phytochromes is that with a PCM coupled to a histidine kinase, but combinations with GGDEF, EAL, PAS and STAS domains are also possible. Bathy phytochromes, which in contrast to other phytochromes have a Pfr ground state or dark adapted state (Fig. 1), are found in a separate group; these proteins are also characterized by a C-terminal response regulator as an intrinsic module (37). This broad diversity of bacterial phytochromes reflects the overall diversity of bacterial proteins which arose during an evolution of 3.5 billion years. Phytochromes of eukaryotic groups, which are fungi, heterokonts (including diatoms) and archaeplastida (comprising the plants), are less diverse (24,38,39). All plant phytochromes are of the PCM-PAS-PAS-histidine kinase type (Fig. 3), except the neochromes that exhibit some domain rearrangement. Fungal phytochromes show a PCM-histidine kinase-response regulator domain arrangement (Fig. 3). The archaeplastida and the fungi form clear monophyletic groups (22,24,38,39); within the group of plant phytochromes, the PhyA/C and PhyB/C/D branches can be clearly distinguished. An evolutionary hallmark is the chromophore-binding Cys residue. This Cys is found in the N-terminus of the PAS domain in those phytochromes which have a biliverdin (BV) chromophore (see Fig. 1 for chromophore

structure and Fig. 3 for domain arrangement), that is, most bacterial, fungal and heterokont phytochromes. *Agrobacterium* Agp1 was in fact the first phytochrome for which this binding site was identified by mutagenesis (32) and mass spectrometry (40). If phytochromobilin (PϕB) or phycocyanobilin (PCB) is used as chromophore (see Fig. 1 for structures), the chromophore-binding Cys lies in the GAF domain. In both cases is the respective Cys highly conserved, and it is also mutually exclusive (40). The choice of a bilin with a ring A ethylidene side chain as chromophore and the chromophore-binding Cys in the GAF domain correlate in archaeplastida and typical cyanobacterial phytochromes. This speaks for a cyanobacterial origin of archaeplastida phytochromes and thus for an engulfment of the phytochrome gene *via* the plastid endosymbiont. However, a change of a single amino acid could as well have happened independently—in the cyanobacterial and in the archaeplastida lines. It has indeed been reported several times that the introduction of a cysteine at the right position of the GAF domain of a BV-binding phytochrome results in covalent attachment of a PCB chromophore (11,32). In most published phylogenetic trees, plant phytochromes do not appear as subgroup of cyanobacterial phytochromes (22,39). The construction of a phylogenetic tree has many degrees of freedom: choice of sequences, alignment algorithms and parameters, or choice of phylogeny program and the respective parameters. All these vary from one study to the other. We have constructed many different trees using different algorithms in order to improve the quality of the predictions. In many cases, we obtained trees in which cyanobacterial and archaeplastida phytochromes appeared as sister groups, as long as the trees were constructed with the PCM sequences. A tree in which such a relationship is given is shown in Fig. 4. We therefore favor a close phylogenetic relationship between archaeplastidal and plant phytochromes. This is in line with a pathway *via* primary endosymbiosis. In studies where the archaeplastidal phytochromes branch at other positions of the phylogenetic tree, the bacterial groups closest to the archaeplastida consistently differ between individual studies. In other words, there is no consensus alternative to the cyanobacteria that would be supported by two independent studies. Such studies are probably based on misalignments or other "errors".

The histidine kinase modules of phytochromes can also be used for phylogenetic studies, because most phytochromes have such modules or share some homologies with these. Our results show a completely different evolutionary pattern for the histidine kinase (see Fig. 4 as example). In those analyses we never observed a close relationship between plants and cyanobacteria. Our conclusion was that the PCMs and histidine kinase modules have undergone several rearrangements in the evolution (24). Such a rearrangement can explain the insertion of two PAS domains between PCM and histidine kinase as found in plant phytochromes. There are many protein sequences in the databases with multiple PAS domains and a histidine kinase (see bottom of Fig. 3 as example). A fusion of the phytochrome PCM with a fragment of such a protein could have generated the first typical plant phytochrome.

The origin of the other eukaryotic phytochrome PCMs can be discussed in a similar manner. Heterokonts (encompassing diatoms and brown algae) are derived from secondary endosymbiosis (41). These phytochromes could either derive from the primary (cyanobacterial) and the secondary endosymbiont (probably red alga) or from the host of this endosymbiont. The latter alternative is the more likely one because heterokont phytochromes have a BV-binding site (33), and in phylogenetic analyses they never appear related to cyanobacterial or archaeplastidal phytochromes. The domain arrangement with a C-terminal response regulator domain points also to a rearrangement of PCM and C-terminus. Bacterial phytochromes with an intrinsic response regulator domain have also a HWE histidine kinase domain, which is not too closely related to the corresponding domains in heterokont phytochromes.

As fungi do not have plastids and are also not derived from ancestors that contained a plastid, the pathway *via* plastid endosymbiosis was not possible. Accordingly, these phytochromes also have a BV-binding site and a C-terminal response regulator domain, a chromophore and a domain arrangement as found predominantly in non-cyanobacterial bacterial species. Fungal and heterokont phytochromes could have the same prokaryotic origin, and in a recent study, they do indeed appear as sister groups (33). The last eukaryotic group which has phytochromes, the amoebozoa, encompasses the slime molds (42,43). This group is the sister group of ophistokonts in which fungi, animals and few other subgroups are united. The evolutionary position of slime mold phytochromes would therefore be highly interesting. Presently two slime mold phytochrome sequences are known, both from *Physarum polycephalum* (11,42). In our own preliminary studies, however, it was not possible to perform reliable alignments with these sequences.

PHYTOCHROMES OF *AGROBACTERIUM FABRUM*

The positions of Agp1 and Agp2 in the phylogenetic trees are indicated by blue boxes in Fig. 4. The two phytochromes of *A. fabrum* are phylogenetically not closely related to each other. Agp1 is a normal bacterial phytochrome with a prototypical domain arrangement. Depending on the topic, it can either be taken as representative of the majority of bacterial phytochromes which have a Pr ground state and a light regulated His kinase, or as a model for all phytochromes, if the mechanism underlying intramolecular signal transduction within the PCM is considered. The unusual domain arrangement of Agp2 with a HWE histidine kinase and a response regulator is found in several other phytochromes of rhizobiales (37), a group of related α-proteobacteria that live in the soil. As noted above, Agp2 belongs to the bathy phytochromes which have a Pfr dark form (Fig. 1). In our phylogenetic studies, the PCM and the histidine kinase module of Apg2 are placed quite at the base of the trees (Fig. 4); Agp2 could be an ancient form of bacterial phytochromes.

BIOLOGICAL FUNCTIONS

Phytochromes have been discovered in plants, where they are the dominating photoreceptors that participate in the control of almost any light dependent developmental step (44); seed germination, induction of photosynthetic pigments, elongation growth, stomata development to mention just a few examples. Fungal phytochromes that have been discovered later are known to control transition of sexual to asexual development and the induction of stress responses (21,45); phytochrome dependent responses of diatoms and slime molds (43) are also known (33). In comparison to the broad variety of phytochromes in bacteria, knowledge of the respective biological responses is rare. The role of cyanobacterial phytochromes is unclear,

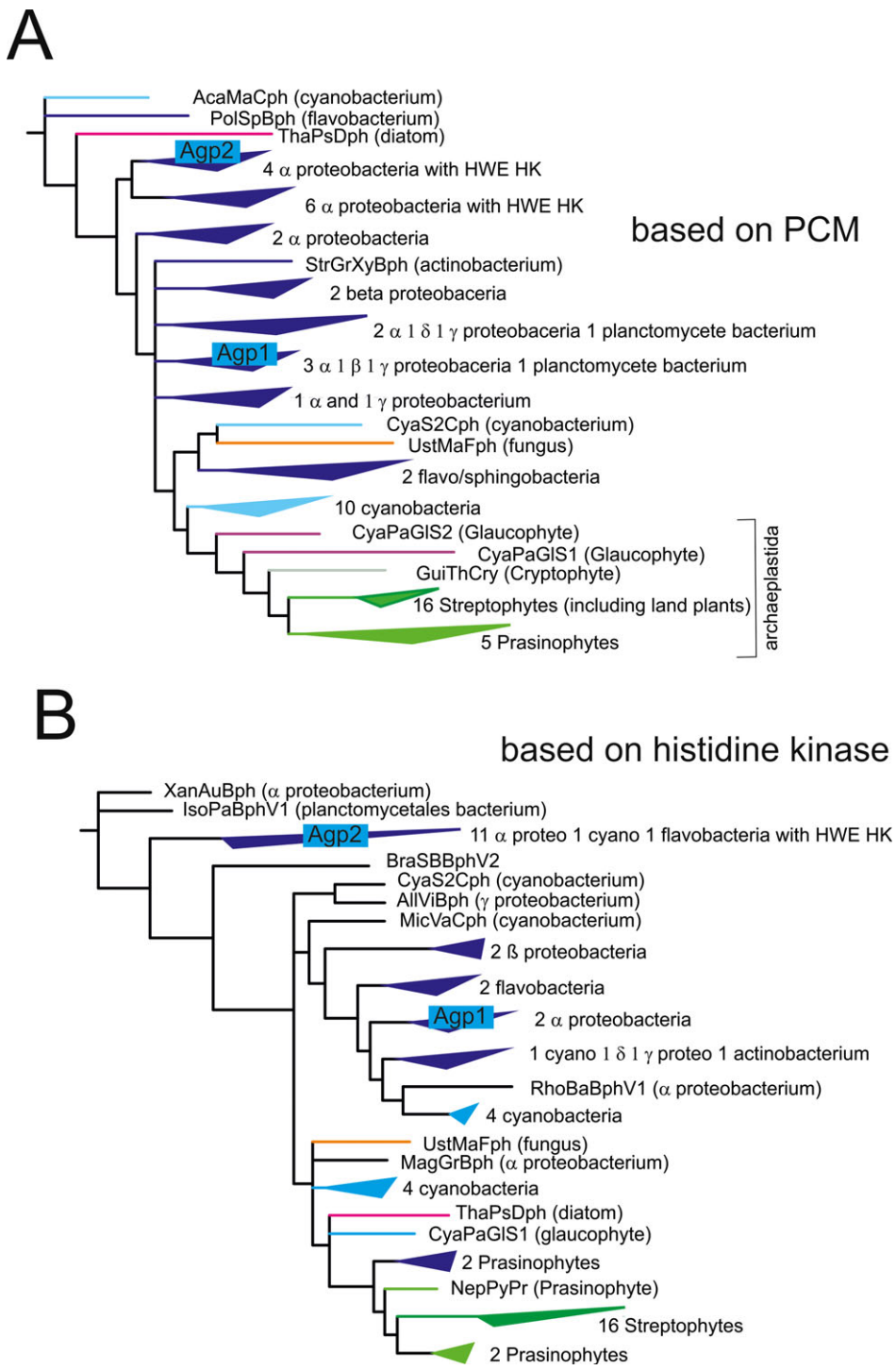

Figure 4. Phylogenetic trees, constructed from PCM (above) or histidine kinase (below) of a selection of 68 phytochrome sequences. The colored triangles stand for clusters of several sequences as given by the text to the right. Single species are indicated by five-letter species abbreviation and a three- to four-letter abbreviation for the respective phytochrome (see (24) for full names). Heterokonts and fungi are represented by *Thalassiosira pseudonana* (ThaPsDph, magenta) and *Ustilago maydis* (UstMaFph, orange), respectively. The alignments were performed by muscle (101) and the trees constructed with MrBayes (102) 3.24 (WAG model and approximately 5 000 000 generations). The trees in A and B are based on PCM and histidine kinase regions, respectively (38). The light blue textboxes indicate the subgroups in which *Agrobacterium fabrum* phytochromes Agp1 and Agp2 appear.

although many responses controlled by cyanobacteriochromes are known. In prokaryotes, the first phytochrome effect was found in photosynthetic proteobacteria. The synthesis of bacteriochlorophyll and photosystem complexes is light regulated *via* phytochrome in *Bradyrhizobium* and *Rhodopseudomonas palustris* species (46). *Bradyrhizobium* and *Agrobacterium* share a closer relationship within the Rhizobiales. Other related phytochrome effects have been found in these bacteria (47) and the swarming of *Pseudomonas syringae* is also mediated by phytochrome (48,49).

In *Agrobacterium fabrum* we have studied light regulation of wild type and mutants of differential gene expression, motility, infectivity (T-DNA transfer from bacterium to plant) and conjugation (plasmid DNA transfer among bacteria). Only eight out of 4500 genes showed differential expression between light and dark. This difference was lost in an agp1^{-} agp2^{-} double mutant (50). A light effect on swimming was attributed to a photolyase which also functions as a photoreceptor here, not to phytochromes (51). Tumor induction of *Arabidospis* root segments was found to be down regulated by red and far-red light, and in phytochrome knockouts, there was very weak infection only. This points to a phytochrome effect on light regulation of infection (50). A clear phytochrome effect was found for the conjugation of *Agrobacterium fabrum*. Driven by results of a computational study (52), a coaction of phytochrome with the TraA protein was suggested (53). Conjugation is a process during which DNA in a single-stranded form is transferred to another cell. TraA is a relaxase which is thought to initiate the formation of single-stranded DNA. Red and far-red light diminished conjugation of *Agrobacterium fabrum* wild type donor cells (see also Fig. 5 as an example (53)). Phytochrome knockout donor strains also showed a reduced DNA transfer efficiency.

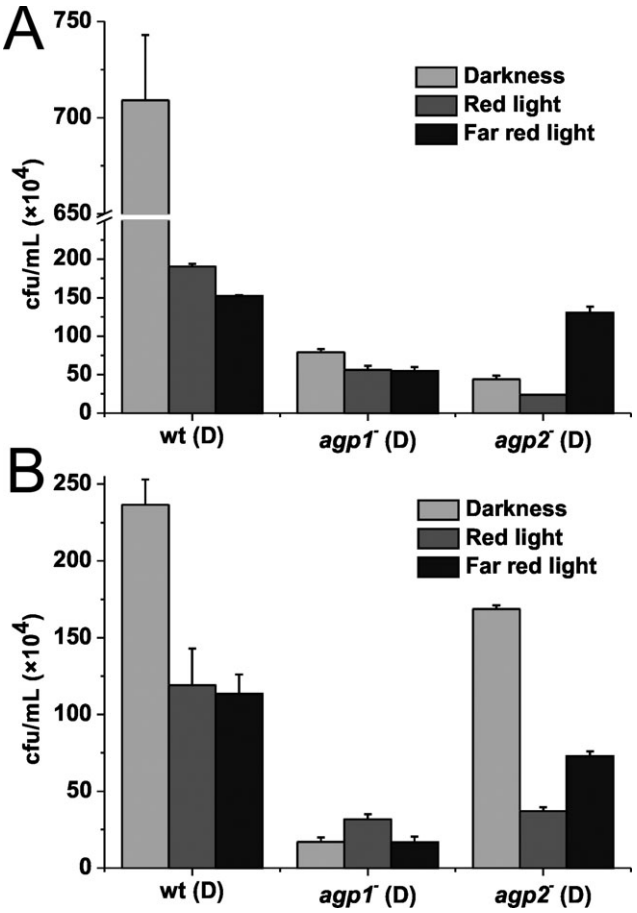

Figure 5. Effects of red and far-red light on conjugation of *Agrobacterium fabrum*. Donor cells (D) with tumor inducing plasmid (Ti-plasmid). The marker plasmid for conjugation is pGUS. (A) Wild-type recipient; (B) agp1$^-$/agp2$^-$ recipient. The number of surviving cells per mL on double selective medium (plasmid in the donor with Kan resistance and recipient with Amp resistance) is given as measure for conjugation efficiency. The figure is drawn after (53).

The double knockout donor did not undergo conjugation at all. The evolutionary advantage of such a light inhibition of conjugation could be a protection against UV damage. Single-stranded DNA is more sensitive against DNA damage than double-stranded DNA, because the most efficient repair requires the complementary strand—conjugation is one example in which DNA is in a single-stranded mode. The T-DNA transfer to plant cells occurs also in a single-stranded mode. Although the effect of Agp1 and Agp2 on differential gene expression in *Agrobacterium fabrum* seems much less prominent than in plants or fungi, both phytochrome effects are processes in which DNA, but solely plasmid DNA, is processed.

BIOCHEMICAL STUDIES

Both Agp1 and Agp2 have been subject of a number of biochemical and biophysical studies. Using locked chromophores, the stereochemistry of the chromophores in the Pr and Pfr states of Agp1 and Agp2 was proposed to be *ZZZssa* for Pr and *ZZEssa* for Pfr (54–57). (A cartoon on the universal phytochrome photocycle and the stereochemistry of the chromophore in the Pr and Pfr forms is depicted in Fig. 2.) Adducts with locked chromophores that cannot undergo stereochemical changes at the methine bridge between rings A and B exhibit light-induced spectral changes, but the spectra of the photoproducts differ largely from Pfr (56,58). Therefore, structural changes involving ring A are probably also required during photoconversion. Rearrangements of the local environment around ring A are also postulated by fluorescein labeling at the chromophore-binding Cys20 of Agp1, combined with time-resolved spectroscopy: spectral changes in fluorescein were observed upon chromophore incorporation and by photoconversion (59). These measurements can be correlated with proton release and uptake that has also been measured using fluorescein as indicator (60). During Pr-Pfr photoconversion, proton release is related to the formation of meta-Rc and proton reuptake corresponds with the meta-Rc to Pfr transition. Polarity change of the ring A environment is also observed during the meta-Rc to Pfr transition.

The early time steps that lead to the formation of Pfr have been investigated for both Agp1 and Agp2 by ultrafast spectroscopy (61–63). During measurements on the Agp1 Pfr to Pr photoconversion an interesting and yet unresolved observation was made. The overall photoconversion from Pfr to Pr was found to have a very low quantum yield of 0.4% (32), whereas the quantum yield for photoisomerization, the first step in Pfr-Pr conversion, was found to be in the same range as observed for other phytochromes (63). It therefore seems that after *E-Z* photoisomerization, a major fraction of chromophores isomerizes back to the *E* configuration. The chromphore structures in the Pfr states of various bathy and prototypical biliverdin-binding phytochromes were studied in more detail using a combined spectroscopic-theoretical approach (64). A special feature of the bathy phytochrome Agp2 is its spectral property in the Pr form. Unlike other phytochromes, the Pr spectra are pH sensitive, indicating chromophore deprotonation at alkaline pH (65). A reaction scheme starting from the excited state of the Pr chromophore for Agp2 under acidic/alkaline conditions was deduced from the ultrafast measurements (61). Within 1.5/6 ps after excitation a twist around C5 of the chromophore is induced. During the next 22/58 ps another twist around C15 occurs; during this step the deprotonated chromophore becomes protonated at alkaline pH.

From here, the *Z-E* isomerization to lumi-R or the back reaction to Pr occurs. This bifurcation of the reaction pathway and the distribution between both pathways are the determinants of the photoconversion quantum yield.

Proton exchange reactions during photoconversion were also analyzed by Resonance Raman spectroscopy in solution (65–67) and on crystals (68). In a recent study on the bathy phytochromes Agp2 and *Pseudomonas aeruginosa* phytochrome PaBphP, a proton exchange reaction between a conserved histidine and the chromophore was found which enables a keto enol tautomerism of ring D that drives the thermal back reaction (dark reversion) from Pr to Pfr (69).

An interesting temperature effect on kinase activity and spectral properties was found for Agp1: with increasing temperature from 20°C to 35°C the autophosphorylation activity dropped to almost zero. The maximum activity is found at 20–25°C (70,71). A similar effect was observed in cyanobacterial phytochrome Cph1 but with a temperature optimum at 5°C; that is, the colder the temperature, the more active the kinase. The tested temperatures are in the physiological range; thus, the observed effect can be expected to be relevant for the *in vivo* situation as well. Such a temperature effect has also been described for other histidine kinases such as the VirA protein that regulates infectivity and motility in *Agrobacterium fabrum* and a thermosensor two-component system of an Antarctic Archaebacterium (72). At 35°C, the photoconversion properties of Agp1 did not follow the general scheme, because besides Pr and Pfr, a third form exists with a bleached Pr-like spectrum that is formed during prolonged irradiation from Pfr. This temperature effect is dependent on the histidine kinase and not found in truncated Agp1-M15. The results imply that phytochrome could not only act as light but also as temperature sensor. In this context, a simple experiment on *Arabidopsis* wild-type and phytochrome mutants was performed to see whether the phytochrome in this plant also responds to temperature. An *Arabidopsis* mutant defective in phytochrome B had a shorter hypocotyl than the wild type when grown at 32°C, but not at 29°C or 23°C. This experiment was performed in darkness (71). It was suggested that plant phytochrome could serve as thermosensor also in darkness (71). Phytochrome-mediated temperature effects in *Arabidopsis* seedlings were indeed found subsequently (73,74).

CRYSTAL STRUCTURE

There is a long list of crystal structures of bacterial phytochromes (see, for example, PDB entries 1ZTU, 2O9C, 2O9B, 3C2W, 3IBR, 3G6O, 3NHQ, 3S7P, 3S7O, 3S7N, 3S7Q, 3NOP, 3NOU, 3NOT, 4IJG, 4O0P, 4O01, 4CQH, 4GW9, 4E04, 4QOJ, 4QOI, 4QOH, 4O8G, 4Y5F, 4Y3I, 4XTQ, 4ZRR, 5Z1W, 5C5K, 5AJG, 5AKP, 4RQ9, 4RPW, 5HSQ, 5I5L, 5LBR, 5L8M, 5K5B, 5MBP, 5MBO), plant phytochrome (PDB entry 4OUR), or cyanobacterial phytochromes (PDB entries 2VEA, 3ZQ5, 3VV4, 4GLQ, 4BWI, 5DFY, 5DFX). These structural data are in some cases supported by electron microscopy (75,76), small angle X-ray scattering (SAXS) (77–79) and NMR measurements on the chromophore (16,80–85) or on the entire protein (PDB entries 2K2N, 2KOI, 2KLI, 2LB9, 2LB5, 2M7U and 2M7V). Almost all crystal structures are from protein fragments and not from full-length proteins. These fragments encompass the PAS-GAF-PHY tridomain or PCM (**P**hotosensory **C**ore **M**odule), PAS-GAF or GAF-PHY domains or, as in the cyanobacteriochromes, GAF domains. One structure of a longer fragment (86) (PDB entry 4E04) and another structure of a full-length phytochrome (87) (PDB entry 5AKP), both with atypical C-terminal domains, are known as well, but there is no full-length structure of a phytochrome that contains a His kinase as part of the C-terminal region. Because there are PCM structures of bathy phytochromes in the Pfr form, normal phytochromes in the Pr form and—in the case of DrBphP—also in both Pr and Pfr forms, structural changes that occur during photoconversion can be well described for the PCM. His kinase structures have on the other hand been obtained from several other model proteins (88). It is nevertheless still unclear how the signal is transmitted from the PCM to other parts of the protein and how, for example, the enzyme activity is modulated.

Three-dimensional structures of homologous proteins or protein domains are always highly similar. This is also true for the protein folds of the different PCMs. The common most relevant features are (also see summary in Table 1): (1) The chromophore pocket is mainly formed by the GAF domain, in which the chromophore-binding amino acids are more conserved than those further apart from the chromophore. The chromophore-binding site of cyanobacterial and plant phytochromes (which bind a phycocyanobilin or phytochromobilin chromophore, respectively) is also part of the GAF domain; (2) The N-terminal PAS domain interacts with the GAF domain in an unusual manner: The N-terminus of the PAS and the N-terminus of the GAF form a so-called figure of eight knot. In cyanobacteriochromes that lack the PAS domain (*e.g.* (89)), such a knot cannot be formed. However, these chromoproteins are also photoactive, indicating that the knot is not required for photoreversibility; (3) In superposed structures, the chromophore-binding Cys of typical bacterial phytochromes (at the N-terminus of the PAS domain) comes very close to the chromophore-binding Cys of plant and cyanobacterial phytochromes. The orientation of the chromophores within the proteins is thus very similar in all PCM structures, no matter which chromophore is incorporated; (4) Crystal structures together with NMR and vibrational spectroscopy confirmed the stereochemistry of the chromophores in Pr and Pfr forms (Fig. 2B) to be the same as suggested by the studies with locked chromophores; (5) The PHY domain may be regarded as a mediating domain in intramolecular signal transduction; it is linked with the histidine kinase or other output domains on its C-terminal end and linked with the chromophore-binding GAF domain at its N-terminus. The so-called tongue of the PHY domain is a region that folds back onto the chromophore pocket, also resulting in an interaction of the PHY with the PAS domain; and (6) Other interesting features of phytochrome structures are the long helices, one connecting GAF and PHY domains and the other connecting the PHY domain with the His kinase module. These helices could have evolved to establish structurally stable domain connections that restrict relative movements of the domains

Table 1. Remarkable features of phytochrome PCM structures.

The protein forms a knot between PAS and GAF
Chromophore embedded in the GAF domain
Chromophore binding Cys in the GAF domain (for PCB or PφB binding) or the PAS domain (for BV binding)
PHY domain forms a tongue that folds back on the chromophore pocket
The stereochemistry of the chromophore is *ZZZssa* in Pr and *ZZEssa* in Pfr

Table 2. Proposed structural differences of phytochrome PCM between Pr and Pfr.

	Pr	Pfr
GAF-PHY connecting helix	Bent	Straight
Base of the tongue	2-stranded antiparallel β-sheet	One α-helix and a loop
Tip of the tongue, Pro 461 (in Agp1)	Interacts with ring A of the chromophore	Interacts with ring D of the chromophore

within narrow ranges and put the domains at their correct positions (although the GAF-PHY connecting helix is not rigid). Moreover, structural changes as triggered by light *via* the chromophore could be stabilized by these long helices, which according to this view should play central roles in intramolecular signal transduction from the sensory module to the output module.

When PCM structures of normal phytochromes in the Pr form and bathy phytochromes in the Pfr form became available, comparative analyses revealed interesting differences in the overall folds and conformations between these two types of proteins (see Table 2 for a summary) (90,91). Based on these observations, it was possible to speculate about conformational changes that occur during Pr-Pfr photoconversion. Crystal structures of *Deinococcus* PCM in the Pr and Pfr forms showed that the observed differences between normal and bathy phytochromes do indeed reflect the protein conformational changes that occur during photoconversion (78,92,93). In the present view, two segments of the tongue that form an antiparallel β-sheet structure in the Pr form swap their positions relative to the GAF domain during photoconversion as described by a "tryptophan switch"

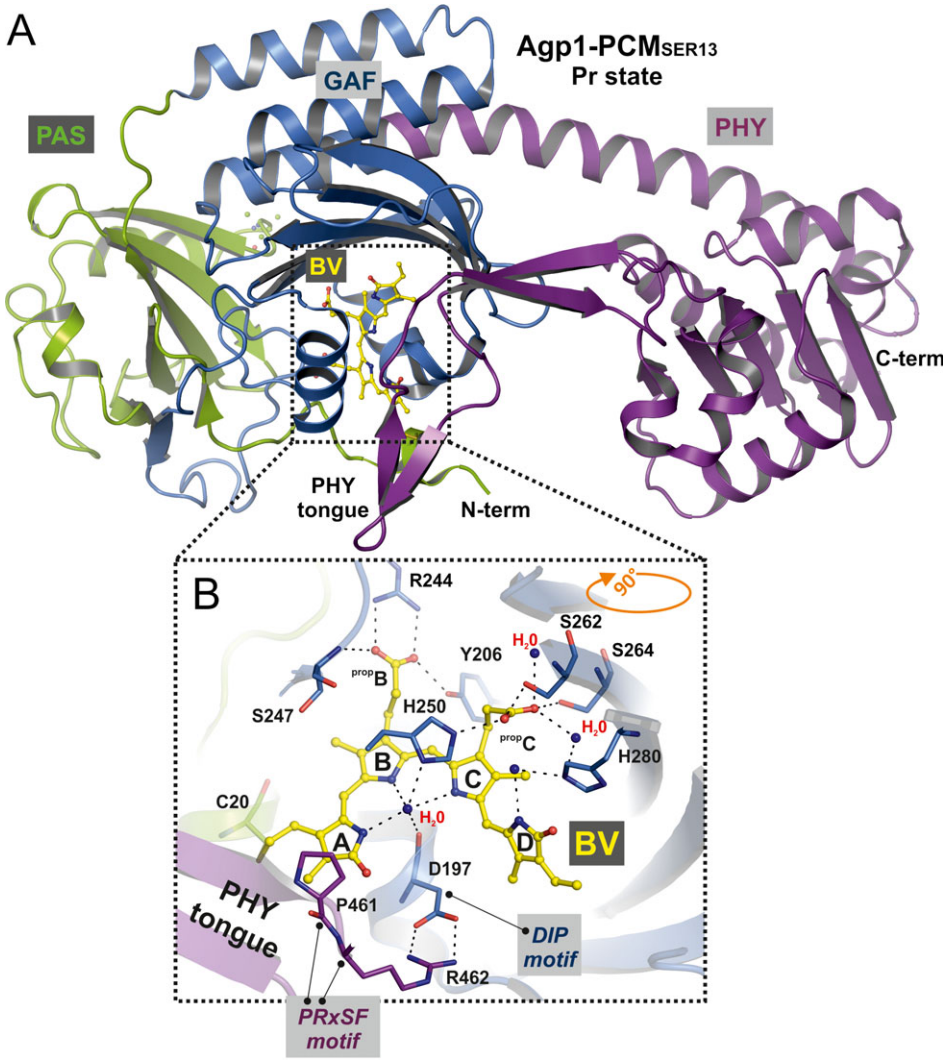

Figure 6. Overall structure of the photosensory core module (PCM) of Agp1 in the Pr state. (A) Ribbon representation of the Agp1-PCM-SER13 monomer. The chromophore biliverdin (BV) and its attachment site Cys20 are shown as balls and sticks and carbon atoms colored in yellow. PAS, GAF and PHY domains are depicted in green, blue and magenta, respectively. (B) Close-up view of the chromophore-binding pocket, relevant amino acids drawn as sticks, potential hydrogen bonding network and relevant water molecules. The four pyrrole rings of biliverdin are labeled A to D, and the propionate side chains of rings B and C are labeled ^{prop}B and ^{prop}C, respectively. The highly conserved *PRxSF* motif of the tongue region from the PHY domain interacts with the chromophore *via* van der Waals interactions between Pro461 and ring A of BV and stabilizes the chromophore-binding pocket by a salt-bridge contact between Arg462 and Asp197 of the highly conserved *DIP* motif (in the GAF domain).

mechanism (89). The same segments refold into an α-helix and a loop during this transition. In addition, the long helix between the GAF and the PHY domain is bent in the Pr and more stretched in the Pfr form.

Although crystals of "Agp1-PCM" diffracting to 3.4 Å resolution were available rather early (94), only a preliminary structural model could be obtained initially as crystallographic refinement was unsatisfactory, even with improved crystals yielding diffraction data sets that were suitable to 2.7 Å resolution (95). A method of protein surface engineering termed "surface entropy reduction" (SER) (96) changed the situation (95). In this approach, clusters of amino acids with long and flexible side chains, Glu and Lys, are replaced by Ala residues to enable the formation of crystal contacts that cannot form with the wild-type protein. Several "SER" mutants yielded similar crystallization results as the wild type, but with the mutant Agp1-SER13-PCM, a combination of two cluster replacements, crystals were obtained under different conditions. With these "Agp1-SER13-PCM" crystals that belonged to a different space group and had different unit cell parameters than the crystals of the wild-type protein, diffraction data could be collected to a resolution of 1.85 Å, which is the best resolution for a PCM crystal so far (Fig. 6). Moreover, using the 3D model of Agp1-SER13-PCM as search model for molecular replacement allowed improving the wild-type Agp1-PCM model significantly such that it could be refined satisfactorily to 2.7 Å resolution. Both crystal structures of Agp1-PCM and Agp1-SER13-PCM differ in the arrangement of two subunits within a dimer. In Apg1-PCM, both subunits are arranged in a parallel manner, whereas an antiparallel arrangement was obtained for Agp1-SER13-PCM (Fig. 7A,B). Apparently, the replacement of amino acids in Agp1-SER13-PCM and the use of different precipitants caused destabilization of the parallel dimer interface while at the same time enabling formation of a new crystal contact, which led to this switch from parallel to antiparallel (95).

The overall structures of the monomers in the crystals of the wild-type and the mutant proteins are very similar, but there are differences at a more detailed level (Fig. 7C). The long helix that connects GAF and PHY domains is more stretched in the Agp1-PCM and more bent in the Agp1-SER13-PCM structure. The different bending must be compensated in another part of the protein because the tip of the tongue interacts with the chromophore pocket of the GAF domain at the same position. This compensation is found in two hinges, one on each side of the tongue itself, next to Trp445 and Trp468, respectively, the two Trp residues that according to the "tryptophan switch" mechanism should swap their roles in packing against the GAF domain after photoconversion. The bending of the long helix is also clearly different between Pr and Pfr crystal structures; in all former cases, the long helix is more bent (Fig. 8). This holds true also for *Deinococcus* phytochrome which has been crystallized in the Pr and Pfr forms (78,92,93). Structural comparisons led to the conclusion that Pr-Pfr photoconversion results in a stretching of the long helix (Fig. 7), combined with a refolding and shortening of the tongue. This view is consistent with the differences observed between the structures of different phytochromes in their dark states, that is, normal phytochromes in the Pr form and bathy phytochromes in the Pfr form (90,91). All Pr and Pfr structures point to a rearrangement of the secondary structure of the tongue. In the Pr form, as in the two Agp1-PCM structures, there are two antiparallel β-strands at the base of the tongue and extended loops (in DrBphP-PCM) or a β-hairpin (*e.g.* in Agp1-SER13-PCM) in the tip of the tongue. In the Pfr form, the tongue folds into an α-helix and an extended loop (Table 2).

The high-resolution structure of Agp1-SER13-PCM shows also a close interaction with Pro461 and the ring A of the chromophore (Fig. 9A). As in the same structure the chromophore adopts a sterically strained conformation at ring A, it was suggested that this steric strain is induced by the interaction with Pro461 which belongs to the conserved *PRxSF* motif in the tip of the tongue (95). A similar steric strain of the chromophore has not been seen in the structures of other phytochromes, but this may be due to the lower resolutions of the respective crystal structure analyses. Consistent with our observation, however, the Pro of the *PRxSF* motif is in van der Waals contact with ring A in all Pr structures. In Pfr structures of other phytochrome PCMs, the homologous Pro residue interacts with ring D of the chromophore (Fig. 9B). There is sufficient evidence to suggest that

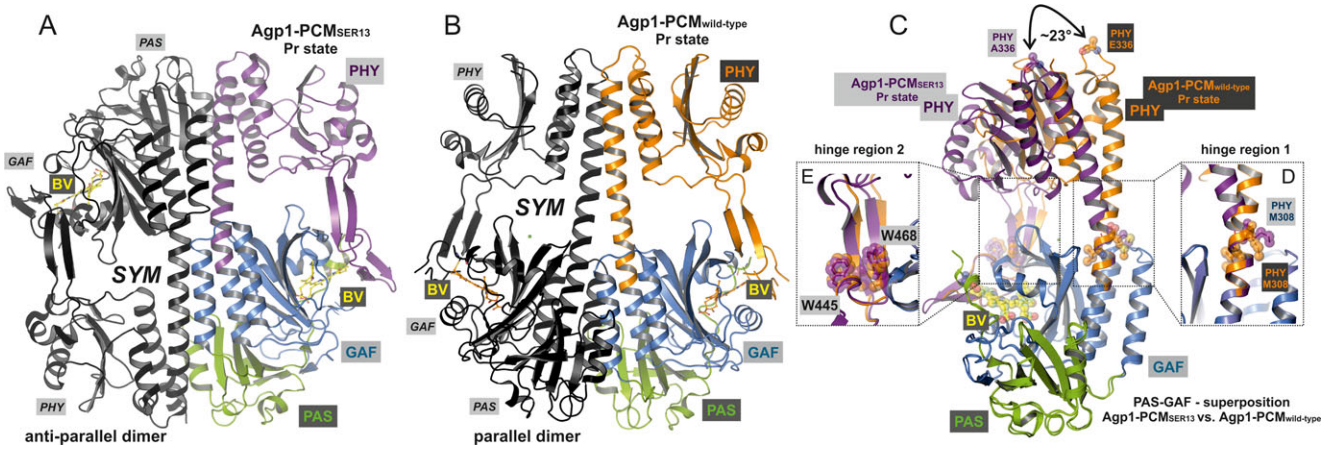

Figure 7. Subunit arrangement in the homo-dimers found in the Agp1-PCM and Agp1-PCM-SER13 crystal structures. (A) Antiparallel arrangement in Agp1-PCM SER13. (B) Parallel arrangement of subunits in Agp1-PCM-SER13. One subunit is drawn with green blue magenta color code for PAS-GAF and PHY domains, respectively, the other subunit in black. (C) Superposition of monomers of Agp1-PCM and Agp1-PCM-SER13. The different bending of the long helix at the GAF-PHY transition is highlighted and the corresponding hinge region 1 shown enlarged in panel D. Panel E shows details of the hinge region 2 of the tongue.

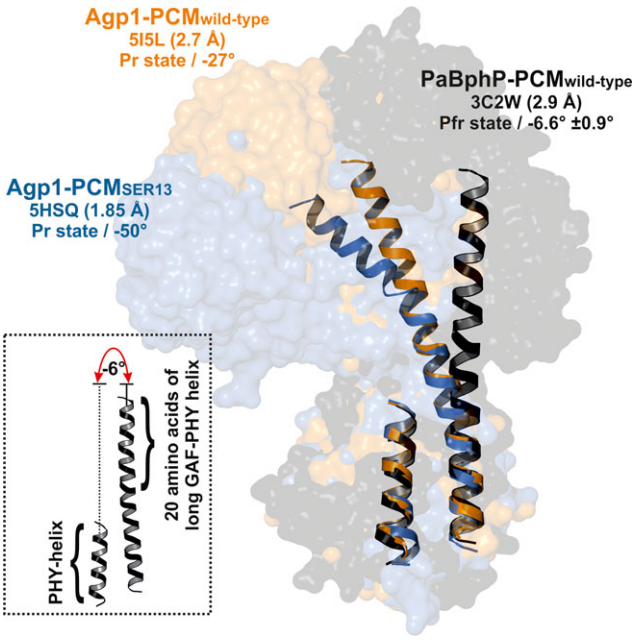

Figure 8. Long GAF-PHY connecting helices in Agp1-SER13-PCM (Pr, PDB entry 5HSQ), Agp1-PCM (Pr, PDB entry 5I5L) and the bathy phytochrome PaBphP (Pfr, PDB entry 3C2W). The bending angles in the hinge region, measured as indicated in the insert and described earlier (95), are given. Almost all Pr and Pfr structures have bent and straight helices, respectively (95).

Pro461 (or its homologs) flips between rings A and D during Pr-Pfr photoconversion. While the Arg and Ser residues of the *PRxSF* motif serve to stabilize the protein conformation in either the Pr or Pfr state (Fig. 9A,B), respectively, we propose that the steric strain induced by the Pro of the same motif in the Pr state drives conversion into the Pfr state after photoexcitation, which is consistent with formation of a bleached photoproduct after red light illumination of the P461A mutant of Agp1 (95). This Pro residue may be regarded as a sensor of initial structural changes in the local environment of pyrrole ring A of the chromophore after photoexcitation of the Pr form. Equally, this residue may sense structural changes caused by photoexcitation of the Pfr state in the ring D environment and drive conversion into Pr.

INTEGRATING RECENT STUDIES ON CONFORMATIONAL CHANGES

As always, new answers impose new questions. Although the structural differences between Pr and Pfr may be considered as settled, it is as yet not clear how these changes are triggered by the light-induced isomerization of the chromophore. A more detailed understanding of the photocycle intermediate structures would be crucial in this regard. The mechanism of signal transmission from the N-terminal PCM to the rest of the protein, for example, the histidine kinase module, and in particular of modulation of histidine kinase activity, is also still unclear. Because typically, phytochromes are homodimeric proteins, changes in the arrangement of both subunits could be important for intramolecular signal transduction. In a recent interdisciplinary study encompassing X-ray crystallography and time-resolved small angle X-ray scattering (SAXS), it has been proposed that within the PCM dimers, the PHY domains separate as a result of Pr to Pfr photoconversion (78,97). It was suggested that the same change of quaternary structure could trigger conformational changes in the His kinase module of the full-length protein. Indeed, the X-ray structures of the DrBphP-PCM in Pr and Pfr (78,92,93) show such a disappearance of the dimer contacts between the PHY domains in the Pfr form. Although both published crystal structures of DrBphP-PCM in the Pfr state or Pfr-enriched state showed a similar Y-shaped subunit arrangement, which was also supported by the SAXS experiments, the Pfr crystal structures of bathy phytochromes exhibit a different subunit arrangement (91). Therefore, without consideration of additional experimental evidence, the subunit arrangements in the PCM crystal structures should not be taken as representative for the structure of the full-length protein in solution. In protein crystal structures, each protein monomer is

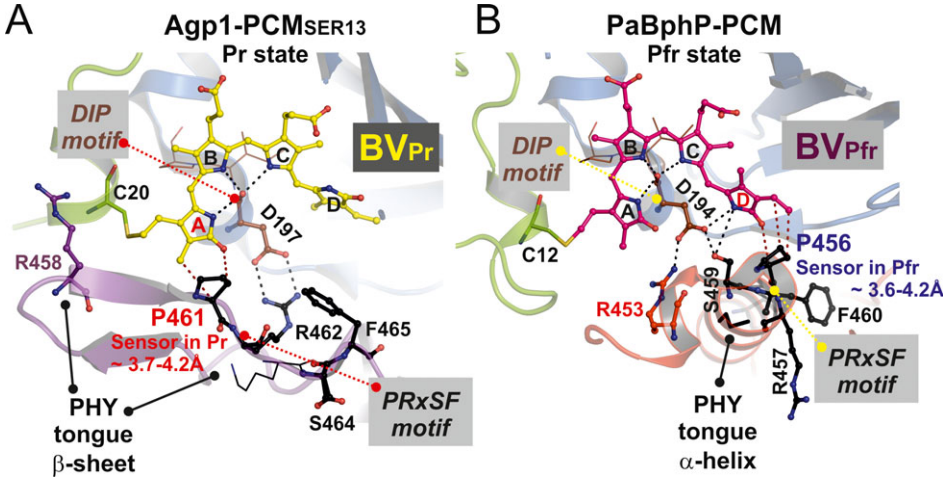

Figure 9. Interactions between residues of the conserved *PRxSF* motif and the chromophore in Pr and Pfr. Pro461 of this motif is in van der Waals contact with ring A of the chromophore in the Pr state of Agp1 and Arg462 stabilizes the protein conformation by a salt bridge with Asp197 of the conserved DIP motif, whereas Ser464 is exposed to the protein surface (A). Of the homologous residues in the *Pseudomonas* phytochrome PaBphP structure in the Pfr state, Pro456 is in van der Waals contact with the carbonyl oxygen of ring D and its side chain, Ser459 participates in hydrogen bonding network that stabilizes the protein conformation, and Arg457 is exposed to the protein surface (B).

always in contact with several other monomers; it is often difficult if not impossible to distinguish between biologically relevant protein–protein interfaces that are part of a quaternary structure and those interfaces which solely exist as crystal contacts. Moreover, there is another discrepancy between the data of Takala *et al.* (78) and former biochemical experiments on the quaternary structures of the cyanobacterial phytochrome Cph1 and of Agp1. The PCM of both bacterial phytochromes was found to be monomeric in the Pr and dimeric in the Pfr form (98–100); Takala *et al.*(78) assumed the DrBphP-PCM to be a dimer in Pr and Pfr. A recent time-resolved SAXS study on full-length DrBphP phytochrome showed indeed a different result for light-induced protein conformational changes (79). According to this new model, the intramolecular signal is relayed by structural changes in the tongue and a twisting of the long helices connecting the PHY domain with the histidine kinase. The large number of degrees of freedom in the modeling of SAXS data demands the use of other structural techniques suitable to characterize light-induced conformational changes in full-length phytochromes. In a recent study on spin-labeled full-length Agp1 (103), distances between two subunits in the dimer were estimated by PELDOR. The position of the spin label was either in the GAF, PHY, or histidine kinase region. These measurements showed that the arrangement of subunits is different from that in the PCM crystal structure, whereas the distances in the histidine kinase region were in agreement with a homology model. No distance changes upon Pr-Pfr photoconversion were found. These results show that the arrangement of subunits does not undergo large changes upon photoconversion. Clearly, for maximal understanding of phytochrome action, more studies on full-length phytochromes are required. Differences between PCMs and full-length proteins should be considered more in the future.

CONCLUSIONS

The phytochrome system of *Agrobacterium fabrum* allows integrated research on light regulation in a bacterium. We know a lot about the biochemical properties of both phytochromes, we know the crystal structure of Agp1-PCM, and we know two biological functions of these photoreceptors. We propose that the different steps in signal transduction can be unraveled in the near future.

Acknowledgements—N.K. and P.S. acknowledge the synchrotrons BESSY-MX/Helmholtz Zentrum Berlin für Materialien und Energie (Joint Berlin MX-Laboratory at the BESSY II electron storage ring (Berlin-Adlershof, Germany)) and the European Synchrotron Radiation Facility (ESRF, Grenoble, France) for continuous support. P.S. acknowledges Charité Universitätsmedizin Berlin for continuous support. P.S. is supported by grants from the Deutsche Forschungsgemeinschaft (SFB740-B6 and SFB1078-B6) and the DFG Cluster of Excellence "Unifying Concepts in Catalysis" (Research Field D3/E3-1).

REFERENCES

1. Gärtner, W. and P. Towner (1995) Invertebrate visual pigments. *Photochem. Photobiol.* **62**, 1–16.
2. Bongards, C. and W. Gärtner (2010) The role of the chromophore in the biological photoreceptor phytochrome: An approach using chemically synthesized tetrapyrroles. *Acc. Chem. Res.* **43**, 485–495.
3. Losi, A., E. Polverini, B. Quest and W. Gärtner (2002) First evidence for phototropin-related blue-light receptors in prokaryotes. *Biophys. J.* **82**, 2627–2634.
4. Holzwarth, A. R., J. Wendler, B. P. Ruzsicska, S. E. Braslavsky and K. Schaffner (1984) Picosecond time-resolved and stationary fluorescence of oat phytochrome highly enriched in the native 124 Kda protein. *Biochim. Biophys. Acta* **791**, 265–273.
5. Schmidt, P., U. H. Westphal, K. Worm, S. E. Braslavsky, W. Gärtner and K. Schaffner (1996) Chromophore-protein interaction controls the complexity of the phytochrome photocycle. *J. Photochem. Photobiol. B* **34**, 73–77.
6. Schulenberg, P. J., M. Rohr, W. Gärtner and S. E. Braslavsky (1994) Photoinduced volume changes associated with the early transformations of bacteriorhodopsin – A laser- induced optoacoustic spectroscopy study. *Biophys. J.* **66**, 838–843.
7. Holzwarth, A. R., E. Venuti, S. E. Braslavsky and K. Schaffner (1992) The phototransformation process in phytochrome: I. Ultrafast fluorescence. *Biochim. Biophys. Acta* **1140**, 59–68.
8. Aramendia, P. F., B. P. Ruzsicska, S. E. Braslavsky and K. Schaffner (1987) Laser flash-photolysis of 124-kilodalton oat phytochrome in H_2O and D_2O solutions – Formation and decay of the I700 intermediates. *Biochemistry* **26**, 1418–1422.
9. Brock, H., B. P. Ruzsicska, T. Arai, W. Schlamann, A. R. Holzwarth, S. E. Braslavsky and K. Schaffner (1987) Fluorescence lifetimes and relative quantum yields of 124-Kilodalton oat phytochrome in H_2O and D_2O solutions. *Biochemistry* **26**, 1412–1417.
10. Lamparter, T., F. Mittmann, W. Gärtner, T. Börner, E. Hartmann and J. Hughes (1997) Characterization of recombinant phytochrome from the cyanobacterium *Synechocystis*. *Proc. Natl Acad. Sci. USA* **94**, 11792–11797.
11. Jorissen, H. J. M. M., B. Quest, A. Remberg, T. Coursin, S. E. Braslavsky, K. Schaffner, N. T. de Marsac and W. Gärtner (2002) Two independent, light-sensing two-component systems in a filamentous cyanobacterium. *Eur. J. Biochem.* **269**, 2662–2671.
12. Quest, B. and W. Gärtner (2004) Chromophore selectivity in bacterial phytochromes: Dissecting the process of chromophore attachment. *Eur. J. Biochem.* **271**, 1117–1126.
13. Quest, B., T. Hübschmann, S. Sharda, N. T. de Marsac and W. Gärtner (2007) Homologous expression of a bacterial phytochrome – The cyanobacterium Fremyella diplosiphon incorporates biliverdin as a genuine, functional chromophore. *FEBS J.* **274**, 2088–2098.
14. Schwinte, P., W. Gärtner, S. Sharda, M. A. Mroginski, P. Hildebrandt and F. Siebert (2008) The photoreactions of recombinant phytochrome CphA from the cyanobacterium Calothrix PCC7601: A low-temperature UV-Vis and FTIR study. *Photochem. Photobiol.* **85**, 239–249.
15. Escobar, F. V., T. Utesch, R. Narikawa, M. Ikeuchi, M. A. Mroginski, W. Gärtner and P. Hildebrandt (2013) Photoconversion mechanism of the second GAF domain of cyanobacteriochrome AnPixJ and the cofactor structure of its green-absorbing state. *Biochemistry* **52**, 4871–4880.
16. Song, C., C. Lang, J. Mailliet, J. Hughes, W. Gärtner and J. Matysik (2012) Exploring chromophore-binding pocket: High-resolution solid-state H-1-C-13 interfacial correlation NMR spectra with windowed PMLG scheme. *Appl. Magn. Reson.* **42**, 79–88.
17. Hill, C., W. Gärtner, P. Towner, S. E. Braslavsky and K. Schaffner (1994) Expression of phytochrome apoprotein from *Avena sativa* in *Escherichia coli* and formation of photoactive chromoproteins by assembly with phycocyanobilin. *Eur. J. Biochem.* **223**, 69–77.
18. Sakamoto, K. and A. Nagatani (1996) Nuclear localization activity of phytochrome B. *Plant J.* **10**, 859–868.
19. Nagatani, K. (2000) Plant biology. Lighting up the nucleus. *Science* **288**, 821–822.
20. Xu, X. S., I. Paik, L. Zhu and E. Huq (2015) Illuminating progress in phytochrome-mediated signaling pathways. *Trends Plant Sci.* **20**, 641–650.
21. Yu, Z. Z., O. Armant and R. Fischer (2016) Fungi use the SakA (HogA) pathway for phytochrome-dependent light signalling. *Nat. Microbiol.* **1**, 5.
22. Duanmu, D. Q., C. Bachy, S. Sudek, C. H. Wong, V. Jimenez, N. C. Rockwell, S. S. Martin, C. Y. Ngan, E. N. Reistetter, M. J. van Baren, D. C. Price, C. L. Wei, A. Reyes-Prieto, J. C. Lagarias and A. Z. Worden (2014) Marine algae and land plants share conserved

phytochrome signaling systems. *Proc. Natl Acad. Sci. USA* **111**, 15827–15832.
23. Rockwell, N. C., D. Duanmu, S. S. Martin, C. Bachy, D. C. Price, D. Bhattacharya, A. Z. Worden and J. C. Lagarias (2014) Eukaryotic algal phytochromes span the visible spectrum. *Proc. Natl Acad. Sci. USA* **111**, 3871–3876.
24. Buchberger, T. and T. Lamparter (2015) Streptophyte phytochromes exhibit an N-terminus of cyanobacterial origin and a C-terminus of proteobacterial origin. *BMC. Res. Notes* **8**, 144.
25. Yoshihara, S., M. Katayama, X. Geng and M. Ikeuchi (2004) Cyanobacterial phytochrome-like PixJ1 holoprotein shows novel reversible photoconversion between blue- and green-absorbing forms. *Plant Cell Physiol.* **45**, 1729–1737.
26. Kehoe, D. M. and A. R. Grossman (1996) Similarity of a chromatic adaptation sensor to phytochrome and ethylene receptors. *Science* **273**, 1409–1412.
27. Hirose, Y., N. C. Rockwell, K. Nishiyama, R. Narikawa, Y. Ukaji, K. Inomata, J. C. Lagarias and M. Ikeuchi (2013) Green/red cyanobacteriochromes regulate complementary chromatic acclimation via a protochromic photocycle. *Proc. Natl Acad. Sci. USA* **110**, 4974–4979.
28. Song, C., F. V. Escobar, X. L. Xu, R. Narikawa, M. Ikeuchi, F. Siebert, W. Gärtner, J. Matysik and P. Hildebrandt (2015) A red/green cyanobacteriochrome sustains its color despite a change in the bilin chromophore's protonation state. *Biochemistry* **54**, 5839–5848.
29. Butler, W. L., K. H. Norris, H. W. Siegelman and S. B. Hendricks (1959) Detection, assay, and preliminary purification of the pigment controlling photoresponsive development of plants. *Proc. Natl Acad. Sci. USA* **45**, 1703–1708.
30. Blumenstein, A., K. Vienken, R. Tasler, J. Purschwitz, D. Veith, N. Frankenberg-Dinkel and R. Fischer (2005) The *Aspergillus nidulans* phytochrome FphA represses sexual development in red light. *Curr. Biol.* **15**, 1833–1838.
31. Hughes, J., T. Lamparter, F. Mittmann, E. Hartmann, W. Gärtner, A. Wilde and T. Börner (1997) A prokaryotic phytochrome. *Nature* **386**, 663.
32. Lamparter, T., N. Michael, F. Mittmann and B. Esteban (2002) Phytochrome from *Agrobacterium tumefaciens* has unusual spectral properties and reveals an N-terminal chromophore attachment site. *Proc. Natl Acad. Sci. USA* **99**, 11628–11633.
33. Fortunato, A. E., M. Jaubert, G. Enomoto, J. P. Bouly, R. Raniello, M. Thaler, S. Malviya, J. S. Bernardes, F. Rappaport, B. Gentili, M. J. J. Huysman, A. Carbone, C. Bowler, M. R. d'Alcala, M. Ikeuchi and A. Falciatore (2016) Diatom phytochromes reveal the existence of far-red-light-based sensing in the ocean. *Plant Cell* **28**, 616–628.
34. Ikeuchi, M. and T. Ishizuka (2008) Cyanobacteriochromes: A new superfamily of tetrapyrrole-binding photoreceptors in cyanobacteria. *Photochem. Photobiol. Sci.* **7**, 1159–1167.
35. Scheerer, P., N. Michael, J. H. Park, S. Nagano, H. W. Choe, K. Inomata, B. Borucki, N. Krauß and T. Lamparter (2010) Light-induced conformational changes of the chromophore and the protein in phytochromes: Bacterial phytochromes as model systems. *ChemPhysChem* **11**, 1090–1105.
36. Gelvin, S. B. (2006) Agrobacterium virulence gene induction. *Methods Mol. Biol.* **343**, 77–84.
37. Rottwinkel, G., I. Oberpichler and T. Lamparter (2010) Bathy phytochromes in rhizobial soil bacteria. *J. Bacteriol.* **192**, 5124–5133.
38. Kooss, S. and T. Lamparter (2016) Cyanobacterial origin of plant phytochromes. *Protoplasma* **254**, 603.
39. Lamparter, T. (2004) Evolution of cyanobacterial and plant phytochromes. *FEBS Lett.* **573**, 1–5.
40. Lamparter, T., M. Carrascal, N. Michael, E. Martinez, G. Rottwinkel and J. Abian (2004) The biliverdin chromophore binds covalently to a conserved cysteine residue in the N-terminus of *Agrobacterium phytochrome* Agp1. *Biochemistry* **43**, 3659–3669.
41. Gould, S. B., R. F. Waller and G. I. McFadden (2008) Plastid evolution. *Annu. Rev. Plant Biol.* **59**, 491–517.
42. Schaap, P., I. Barrantes, P. Minx, N. Sasaki, R. W. Anderson, M. Benard, K. K. Biggar, N. E. Buchler, R. Bundschuh, X. Chen, C. Fronick, L. Fulton, G. Golderer, N. Jahn, V. Knoop, L. F. Landweber, C. Maric, D. Miller, A. A. Noegel, R. Peace, G. Pierron, T. Sasaki, M. Schallenberg-Rudinger, M. Schleicher, R. Singh, T. Spaller, K. B. Storey, T. Suzuki, C. Tomlinson, J. J. Tyson, W. C. Warren, E. R. Werner, G. Werner-Felmayer, R. K. Wilson, T. Winckler, J. M. Gott, G. Glockner and W. Marwan (2015) The *Physarum polycephalum* genome reveals extensive use of prokaryotic two-component and metazoan-type tyrosine kinase signaling. *Genome Biol. Evol.* **8**, 109–125.
43. Lamparter, T. and W. Marwan (2001) Spectroscopic detection of a phytochrome-like photoreceptor in the myxomycete *Physarum polycephalum* and the kinetic mechanism for the photocontrol of sporulation by Pfr. *Photochem. Photobiol.* **73**, 697–702.
44. Chen, M., J. Chory and C. Fankhauser (2004) Light signal transduction in higher plants. *Annu. Rev. Genet.* **38**, 87–117.
45. Bayram, O., G. H. Braus, R. Fischer and J. Rodriguez-Romero (2010) Spotlight on Aspergillus nidulans photosensory systems. *Fungal Genet. Biol.* **47**, 900–908.
46. Giraud, E., J. Fardoux, N. Fourrier, L. Hannibal, B. Genty, P. Bouyer, B. Dreyfus and A. Vermeglio (2002) Bacteriophytochrome controls photosystem synthesis in anoxygenic bacteria. *Nature* **417**, 202–205.
47. Fixen, K. R., A. W. Baker, E. A. Stojkovic, J. T. Beatty and C. S. Harwood (2014) Apo-bacteriophytochromes modulate bacterial photosynthesis in response to low light. *Proc. Natl Acad. Sci. USA* **111**, E237–E244.
48. Wu, L., R. S. McGrane and G. A. Beattie (2013) Light regulation of swarming motility in *Pseudomonas syringae* integrates signaling pathways mediated by a bacteriophytochrome and a LOV protein. *MBio* **4**, e00334–13.
49. Shah, R., G. Pathak, T. Drepper and W. Gärtner (2016) Selective photoreceptor gene knock-out reveals a regulatory role for the growth behavior of *Pseudomonas syringae*. *Photochem. Photobiol.* **92**, 571–578.
50. Rottwinkel, G. (2011) Studien zu Verbreitung, Charakteristika und Funktionen der Bakteriophytochrome in *Rhizobiales*. Ph.D. thesis. KIT Karlsruhe
51. Oberpichler, I., R. Rosen, A. Rasouly, M. Vugman, E. Z. Ron and T. Lamparter (2008) Light affects motility and infectivity of *Agrobacterium tumefaciens*. *Environ. Microbiol.* **10**, 2020–2029.
52. Lamparter, T. (2006) A computational approach to discovering the functions of bacterial phytochromes by analysis of homolog distributions. *BMC Bioinformatics* **7**, 141.
53. Bai, Y., G. Rottwinkel, J. Feng, Y. Liu and T. Lamparter (2016) Bacteriophytochromes control conjugation in *Agrobacterium fabrum*. *J. Photochem. Photobiol., B* **161**, 192–199.
54. Lamparter, T., N. Michael, O. Caspani, T. Miyata, K. Shirai and K. Inomata (2003) Biliverdin binds covalently to *Agrobacterium* phytochrome Agp1 via its ring A vinyl side chain. *J. Biol. Chem.* **278**, 33786–33792.
55. Inomata, K., M. A. S. Hammam, H. Kinoshita, Y. Murata, H. Khawn, S. Noack, N. Michael and T. Lamparter (2005) Sterically locked synthetic bilin derivatives and phytochrome Agp1 from *Agrobacterium tumefaciens* form photoinsensitive Pr- and Pfr-like adducts. *J. Biol. Chem.* **280**, 24491–24497.
56. Inomata, K., S. Noack, M. A. S. Hammam, H. Khawn, H. Kinoshita, Y. Murata, N. Michael, P. Scheerer, N. Krauß and T. Lamparter (2006) Assembly of synthetic locked chromophores with *Agrobacterium* phytochromes Agp1 and Agp2. *J. Biol. Chem.* **281**, 28162–28173.
57. Seibeck, S., B. Borucki, H. Otto, K. Inomata, H. Khawn, H. Kinoshita, N. Michael, T. Lamparter and M. P. Heyn (2007) Locked 5Zs-biliverdin blocks the Meta-R-A to Meta-R-C transition in the functional cycle of bacteriophytochrome Agp1. *FEBS Lett.* **581**, 5425–5429.
58. Inomata, K., H. Khawn, L.-Y. Chen, H. Kinoshita, B. Zienicke, I. Molina and T. Lamparter (2009) Assembly of *Agrobacterium* phytochromes Agp1 and Agp2 with doubly locked bilin chromophores. *Biochemistry* **48**, 2817–2827.
59. Borucki, B. and T. Lamparter (2009) A polarity probe for monitoring light induced structural changes at the entrance of the chromophore pocket in a bacterial phytochrome. *J. Biol. Chem.* **38**, 26005–26016.
60. Borucki, B., D. von Stetten, S. Seibeck, T. Lamparter, N. Michael, M. A. Mroginski, H. Otto, D. H. Murgida, M. P. Heyn and P. Hildebrandt (2005) Light-induced proton release of phytochrome is coupled to the transient deprotonation of the tetrapyrrole chromophore. *J. Biol. Chem.* **280**, 34358–34364.

61. Singer, P., S. Wörner, T. Lamparter and R. Diller (2016) Spectroscopic investigation on the primary photoreaction of bathy phytochrome Agp2-Pr of *Agrobacterium fabrum* somerization in a pH-dependent H-bond network. *ChemPhysChem* **17**, 1288.
62. Schumann, C., R. Groß, N. Michael, T. Lamparter and R. Diller (2007) Sub-picosecond mid-infrared spectroscopy of phytochrome Agp1 from *Agrobacterium tumefaciens*. *ChemPhysChem* **8**, 1657–1663.
63. Schumann, C., R. Groß, M. M. N. Wolf, N. Michael, T. Lamparter and R. Diller (2008) Sub-picosecond mid-infrared spectroscopy of the Pfr reaction of phytochrome Agp1 from *Agrobacterium tumefaciens*. *Biophys. J.* **94**, 3189–3197.
64. Salewski, J., F. Velasquez, S. Kaminski, D. von Stetten, A. Keidel, Y. Rippers, N. Michael, P. Scheerer, P. Piwowarski, F. Bartl, N. Frankenberg-Dinkel, S. Ringsdorf, W. Gärtner, T. Lamparter, M. A. Mroginski and P. Hildebrandt (2013) The structure of the biliverdin cofactor in the Pfr state of bathy and prototypical phytochromes. *J. Biol. Chem.* **288**, 16800.
65. Zienicke, B., I. Molina, R. Glenz, P. Singer, D. Ehmer, F. V. Escobar, P. Hildebrandt, R. Diller and T. Lamparter (2013) Unusual spectral properties of bacteriophytochrome Agp2 result from a deprotonation of the chromophore in the red-absorbing form Pr. *J. Biol. Chem.* **288**, 31738–31751.
66. Piwowarski, P., E. Ritter, K. P. Hofmann, P. Hildebrandt, D. von Stetten, P. Scheerer, N. Michael, T. Lamparter and F. Bartl (2010) Light-induced activation of bacterial Phytochrome Agp1 monitored by static and time-resolved FTIR spectroscopy. *ChemPhysChem* **11**, 1207–1214.
67. von Stetten, D., S. Seibeck, N. Michael, P. Scheerer, M. A. Mroginski, D. H. Murgida, N. Krauss, M. P. Heyn, P. Hildebrandt, B. Borucki and T. Lamparter (2007) Highly conserved residues Asp-197 and His-250 in Agp1 phytochrome control the proton affinity of the chromophore and Pfr formation. *J. Biol. Chem.* **282**, 2116–2123.
68. von Stetten, D., M. Günther, P. Scheerer, D. H. Murgida, M. A. Mroginski, N. Krauß, T. Lamparter, J. Zhang, D. M. Anstrom, R. D. Vierstra, K. T. Forest and P. Hildebrandt (2008) Chromophore heterogeneity and photoconversion in phytochrome crystals and solution studied by resonance Raman spectroscopy. *Angew. Chem. Int. Ed. Engl.* **47**, 4753–4755.
69. Escobar, F. V., P. Piwowarski, J. Salewski, N. Michael, M. F. Lopez, A. Rupp, B. M. Qureshi, P. Scheerer, F. Bartl, N. Frankenberg-Dinkel, F. Siebert, M. A. Mroginski and P. Hildebrandt (2015) A protonation-coupled feedback mechanism controls the signalling process in bathy phytochromes. *Nat. Chem.* **7**, 423–430.
70. Njimona, I. and T. Lamparter (2011) Temperature effects on *Agrobacterium phytochrome* Agp1. *PLoS ONE* **6**, e25977.
71. Njimona, I., R. Yang and T. Lamparter (2014) Temperature effects on bacterial phytochrome. *PLoS ONE* **9**, e109794.
72. Najnin, T., K. S. Siddiqui, T. Taha, N. Elkaid, G. Kornfeld, P. M. G. Curmi and R. Cavicchioli (2016) Characterization of a temperature-responsive two component regulatory system from the Antarctic archaeon, *Methanococcoides burtonii*. *Sci. Rep.* **6**, 27162.
73. Legris, M., C. Klose, E. S. Burgie, C. Costigliolo, M. Neme, A. Hiltbrunner, P. A. Wigge, E. Schafer, R. D. Vierstra and J. J. Casal (2016) Phytochrome B integrates light and temperature signals in Arabidopsis. *Science* **354**, 897–900.
74. Jung, J. H., M. Domijan, C. Klose, S. Biswas, D. Ezer, M. Gao, A. K. Khattak, M. S. Box, V. Charoensawan, S. Cortijo, M. Kumar, A. Grant, J. C. Locke, E. Schafer, K. E. Jaeger and P. A. Wigge (2016) Phytochromes function as thermosensors in Arabidopsis. *Science* **354**, 886–889.
75. Burgie, E. S., T. Wang, A. N. Bussell, J. M. Walker, H. L. Li and R. D. Vierstra (2014) Crystallographic and electron microscopic analyses of a bacterial phytochrome reveal local and global rearrangements during photoconversion. *J. Biol. Chem.* **289**, 24573–24587.
76. Li, H., J. R. Zhang, R. D. Vierstra and H. L. Li (2010) Quaternary organization of a phytochrome dimer as revealed by cryoelectron microscopy. *Proc. Natl Acad. Sci. USA* **107**, 10872–10877.
77. Vaidya, A. T., D. Top, C. C. Manahan, J. M. Tokuda, S. Zhang, L. Pollack, M. W. Young and B. R. Crane (2013) Flavin reduction activates Drosophila cryptochrome. *Proc. Natl Acad. Sci. USA* **110**, 20455–20460.
78. Takala, H., A. Björling, O. Berntsson, H. Lehtivuori, S. Niebling, M. Hoernke, I. Kosheleva, R. Henning, A. Menzel, J. A. Ihalainen and S. Westenhoff (2014) Signal amplification and transduction in phytochrome photosensors. *Nature* **509**, 245–248.
79. Björling, A., O. Berntsson, H. Lehtivuori, H. Takala, A. J. Hughes, M. Panman, M. Hoernke, S. Niebling, L. Henry, R. Henning, I. Kosheleva, V. Chukharev, N. V. Tkachenko, A. Menzel, G. Newby, D. Khakhulin, M. Wulff, J. A. Ihalainen and S. Westenhoff (2016) Structural photoactivation of a full-length bacterial phytochrome. *Sci. Adv.* **2**, e1600920.
80. Song, C., L. O. Essen, W. Gärtner, J. Hughes and J. Matysik (2012) Solid-state NMR spectroscopic study of chromophore-protein interactions in the Pr ground state of plant phytochrome A. *Mol. Plant* **5**, 698–715.
81. Song, C., G. Psakis, C. Lang, J. Mailliet, W. Gärtner, J. Hughes and J. Matysik (2011) Two ground state isoforms and a chromophore D-ring photoflip triggering extensive intramolecular changes in a canonical phytochrome. *Proc. Natl Acad. Sci. USA* **108**, 3842–3847.
82. Rohmer, T., C. Lang, C. Bongards, K. B. S. S. Gupta, J. Neugebauer, J. Hughes, W. Gärtner and J. Matysik (2010) Phytochrome as molecular machine: Revealing chromophore action during the Pfr -> Pr photoconversion by magic-angle spinning NMR spectroscopy. *J. Am. Chem. Soc.* **132**, 4431–4437.
83. Roben, M., J. Hahn, E. Klein, T. Lamparter, G. Psakis, J. Hughes and P. Schmieder (2010) NMR spectroscopic investigation of mobility and hydrogen bonding of the chromophore in the binding pocket of phytochrome proteins. *ChemPhysChem* **11**, 1248–1257.
84. Hahn, J., H. M. Strauss and P. Schmieder (2008) Heteronuclear NMR investigation on the structure and dynamics of the chromophore binding pocket of the cyanobacterial phytochrome Cph1. *J. Am. Chem. Soc.* **130**, 11170–11178.
85. Hahn, J., R. Kuhne and P. Schmieder (2007) Solution-state (15)N NMR spectroscopic study of alpha-C-phycocyanin: Implications for the structure of the chromophore-binding pocket of the cyanobacterial phytochrome Cph1. *ChemBioChem* **8**, 2249–2255.
86. Bellini, D. and M. Z. Papiz (2012) Structure of a bacteriophytochrome and light-stimulated protomer swapping with a gene repressor. *Structure* **20**, 1436–1446.
87. Otero, L. H., S. Klinke, J. Rinaldi, F. Velazquez-Escobar, M. A. Mroginski, M. Fernandez Lopez, F. Malamud, A. A. Vojnov, P. Hildebrandt, F. A. Goldbaum and H. R. Bonomi (2016) Structure of the full-Length bacteriophytochrome from the plant pathogen *Xanthomonas campestris* provides clues to its long-range signaling mechanism. *J. Mol. Biol.* **428**, 3702–3720.
88. Bhate, M. P., K. S. Molnar, M. Goulian and W. F. DeGrado (2015) Signal transduction in histidine kinases: Insights from new structures. *Structure* **23**, 981–994.
89. Anders, K., G. Daminelli-Widany, M. A. Mroginski, D. von Stetten and L. O. Essen (2013) Structure of the cyanobacterial phytochrome 2 photosensor implies a tryptophan switch for phytochrome signaling. *J. Biol. Chem.* **288**, 35714–35725.
90. Essen, L. O., J. Mailliet and J. Hughes (2008) The structure of a complete phytochrome sensory module in the Pr ground state. *Proc. Natl Acad. Sci. USA* **105**, 14709–14714.
91. Yang, X., J. Kuk and K. Moffat (2008) Crystal structure of *Pseudomonas aeruginosa* bacteriophytochrome: Photoconversion and signal transduction. *Proc. Natl Acad. Sci. USA* **105**, 14715–14720.
92. Burgie, E. S., J. Zhang and R. D. Vierstra (2016) Crystal structure of deinococcus phytochrome in the photoactivated state reveals a cascade of structural rearrangements during photoconversion. *Structure* **24**, 448–457.
93. Burgie, E. S., A. N. Bussell, J. M. Walker, K. Dubiel and R. D. Vierstra (2014) Crystal structure of the photosensing module from a red/far-red light-absorbing plant phytochrome. *Proc. Natl Acad. Sci. USA* **111**, 10179–10184.
94. Scheerer, P., N. Michael, J. H. Park, S. Noack, C. Forster, M. A. S. Hammam, K. Inomata, H. W. Choe, T. Lamparter and N. Krauß (2006) Crystallization and preliminary X-ray crystallographic analysis of the N-terminal photosensory module of phytochrome Agp1, a biliverdin-binding photoreceptor from Agrobacterium tumefaciens. *J. Struct. Biol.* **153**, 97–102.

95. Nagano, S., P. Scheerer, K. Zubow, N. Michael, K. Inomata, T. Lamparter and N. Krauß (2016) The crystal structures of the N-terminal photosensory core module of agrobacterium phytochrome agp1 as parallel and anti-parallel dimers. *J. Biol. Chem.* **291**, 20674–20691.
96. Derewenda, Z. S. (2004) Rational protein crystallization by mutational surface engineering. *Structure* **12**, 529–535.
97. Bjorling, A., O. Berntsson, H. Takala, K. D. Gallagher, H. Patel, E. Gustavsson, R. St Peter, P. Duong, A. Nugent, F. Zhang, P. Berntsen, R. Appio, I. Rajkovic, H. Lehtivuori, M. R. Panman, M. Hoernke, S. Niebling, R. Harimoorthy, T. Lamparter, E. A. Stojkovic, J. A. Ihalainen and S. Westenhoff (2015) Ubiquitous structural signaling in bacterial phytochromes. *J. Phys. Chem. Lett.* **6**, 3379–3383.
98. Strauss, H. M., P. Schmieder and J. Hughes (2005) Light-dependent dimerisation in the N-terminal sensory module of cyanobacterial phytochrome 1. *FEBS Lett.* **579**, 3970–3974.
99. Esteban, B., M. Carrascal, J. Abian and T. Lamparter (2005) Light-induced conformational changes of cyanobacterial phytochrome Cph1 probed by limited proteolysis and autophosphorylation. *Biochemistry* **44**, 450–461.
100. Noack, S. and T. Lamparter (2007) Light modulation of histidine-kinase activity in bacterial phytochromes monitored by size exclusion chromatography, crosslinking, and limited proteolysis. *Methods Enzymol.* **423**, 203–221.
101. Edgar, R. C. (2004) MUSCLE: Multiple sequence alignment with high accuracy and high throughput. *Nucleic Acids Res.* **32**, 1792–1797.
102. Ronquist, F., M. Teslenko, P. van der Mark, D. L. Ayres, A. Darling, S. Hohna, B. Larget, L. Liu, M. A. Suchard and J. P. Huelsenbeck (2012) MrBayes 3.2: Efficient bayesian phylogenetic inference and model choice across a large model space. *Syst. Biol.* **61**, 539–542.
103. Kacprzak, S., I. Njimona, A. Renz, J. Feng, E. Reijerse, W. Lubitz, N. Krauß, P. Scheerer, S. Nagano, T. Lamparter and S. Weber (2017) Inter-subunit distances in full-length, dimeric, bacterial phytochrome Agp1, as measured by PELDOR between different spin label positions, remain unchanged upon photoconversion. *J. Biol. Chem*. doi:10.1074/jbc.M116.761882.

AUTHOR BIOGRAPHIES

Tilman Lamparter was born 1959 in Sindelfingen, Germany. He studied Biology in Tübingen and performed his Diploma thesis on the "Zea paradoxon" in the group of Eberhard Schäfer in Freiburg and his PhD thesis on the membrane association of plant phytochrome in the group of Rainer Hertel in Freiburg. In 1992, he was a Post Doc in Dr. Elmar Hartmann's lab in the Plant Physiology Department at the Freie Universität Berlin, where he continued to work as a project leader until 2007. He has been on several research visits to work with Vitally Sineshchekov (Moscow), David Cove (Leeds, England) and Masamitsu Wada (Tokyo and Okazaki) to study phytochrome biochemistry and physiological action in moss cells. In 2000, he started a research collaboration with Norbert Krauß. Since 2007, he has been a professor of Botany at the Karlsruhe Institute of Technology. His current interest is on the biochemistry of bacterial phytochromes, photolyases and cyanobacteria based biotechnology.

Norbert Krauß was born 1960 in Cologne, Germany. He did his PhD in the field of structural inorganic chemistry at the University of Cologne under the supervision of Karl-Friedrich Tebbe before he joined the groups of Wolfram Saenger and Horst Tobias Witt in Berlin in 1989. In Berlin, he was a major contributor to the high-resolution structure analysis of cyanobacterial photosystem I and was also involved in the work leading to the first crystal structure of photosystem II, both published in 2001. In 2000, he started a collaboration with Tilman Lamparter and Jon Hughes on bacterial phytochromes and moved to the "Charité" in Berlin. From 2007 to 2015, Norbert Krauß was Senior Lecturer in Structural Biology at Queen Mary University of London. In 2016, he joined Tilman Lamparter's group at the Karlsruhe Institute of Technology. His current major research interests are in photoreceptors, DNA photolyases, and proteins involved in the light reactions of photosynthesis.

Patrick Scheerer, born 1973 in Kirchen/Sieg, Germany, studied biophysics at the Humboldt-Universität of Berlin, Germany. He obtained his PhD in 2012 for the scientific work on crystal structures of the activated G-protein coupled receptor rhodopsin with his supervisor Prof. Klaus Peter Hofmann at the Charité – Universitätsmedizin Berlin and at the Technische Universität Berlin (TUB). After his dissertation he established his own research group "Protein X-ray Crystallography & Signal Transduction" at the Institute of Medical Physics and Biophysics – Charité in Berlin. He accepted a permanent position as research group leader at Charité – Universitätsmedizin Berlin in 2014. His centers of interest are to understand the functional and structural basis of signal transduction in G-protein coupled receptors, photoreceptors and metallo-proteins.